

# Water Hydrogen Bond Dynamics in Aqueous Solutions of Amphiphiles

Guillaume Stirnemann,<sup>†</sup> James T. Hynes,<sup>†,‡</sup> and Damien Laage<sup>\*,†</sup>

Chemistry Department, Ecole Normale Supérieure, UMR ENS-CNRS-UPMC 8640, rue Lhomond, 75005 Paris, France and Department of Chemistry and Biochemistry, University of Colorado, Boulder, Colorado 80309-0215

Received: December 10, 2009; Revised Manuscript Received: January 15, 2010

The hydrogen bond dynamics of water in a series of amphiphilic solute solutions are investigated through simulations and analytic modeling with an emphasis on the interpretation of experimentally accessible two-dimensional infrared (2D IR) photon echo spectra. We evidence that for most solutes the major effect in the hydration dynamics comes from the hydrophilic groups. These groups can retard the water dynamics much more significantly than can hydrophobic groups by forming strong hydrogen bonds with water. By contrast, hydrophobic groups are shown to have a very moderate effect on water hydrogen bond breaking kinetics. We also present the first calculation of the 2D IR spectra for these solutions. While 2D IR spectroscopy is a powerful technique to probe water hydrogen bond network fluctuations, interpretations of aqueous solution spectra remain ambiguous. We show that a complementary approach through simulations and calculation of the spectra lifts the ambiguity and provides a clear connection between the simulated molecular picture and the experimental spectroscopy data. For amphiphilic solute solutions, we show that, in contrast with techniques such as NMR or ultrafast anisotropy, 2D IR spectroscopy can discriminate between waters next to the solutes hydrophobic and hydrophilic groups. We also evidence that the water dynamics slowdown due to the hydrophilic groups is dramatically enhanced in the 2D IR spectral relaxation, because these groups can induce a slow chemical exchange with the bulk, even when recognized exchange signatures are absent. Implications for the understanding of water around chemically heterogeneous systems such as protein surfaces and for the interpretation of 2D IR spectra in these cases are discussed.

## I. Introduction

Water dynamics plays a central role in many fundamental chemical and biochemical processes. For chemical reactions in aqueous solutions, the reacting solutes' covalent bond breaking and forming processes lead to charge redistribution. A major component of the dynamic coupling of this redistribution to the water solvent molecules involves the reorganization of the latter's hydrogen (H)-bonds, itself connected to the reorientation of water dipoles. For example, in two fundamental mechanisms,  $S_N2$ <sup>1</sup> and proton transfer<sup>2–5</sup> reactions in aqueous solution, a crucial feature is the rearrangement of the surrounding water molecules; the new arrangement of the water dipoles produces an electric field that favors the product charge distribution, and this reorganization constitutes a crucial component for the reaction mechanism and rate. In biochemical processes, the central role of water dynamics in myriad arenas is beginning to be recognized.<sup>6</sup> Beyond the participation of water molecules in the chemical step of numerous enzyme catalyses,<sup>6</sup> water acts as a lubricant during enzyme catalysis to facilitate the necessary conformational transitions.<sup>6</sup> In proton pump proteins such as bacteriorhodopsin, a hydrogen-bonded chain of internal waters channels the proton transfers.<sup>7</sup> Water also plays a key role in DNA structure protection from excess thermal energy.<sup>8</sup> In protein folding, it was recently suggested that water has a dynamic role in mediating the collapse of the proteic chain<sup>9</sup> and that its expulsion from the hydrophobic protein core is part of the rate-limiting step.<sup>10</sup>

Because the behavior of water around a solute differs from that in the bulk, it is therefore critical to understand how the water dynamics is affected by a reactive solute molecule or a biomolecular surface. A key aspect here is that the majority of organic molecules are chemically heterogeneous with hydrophilic and hydrophobic portions (e.g., tert-butyl chloride, organic acids such as phenol, all amino acids). This heterogeneity is more extensive in many biochemical contexts. As an important example, a protein water-exposed surface exhibits great topological disorder and chemical heterogeneity, for instance, through the alternation of hydrophilic and hydrophobic sites. This strongly suggests that one must first understand the hydration dynamics around simpler solutes that will provide insight on the impact of each biomolecular building block on the hydration layer.

Ultrafast infrared spectroscopy is an exquisite experimental tool to investigate water dynamics, since it possesses the required time-resolution to follow the picosecond H-bond network rearrangements. While several recent time-resolved experimental and theoretical investigations have explored the hydration dynamics around hydrophilic ions,<sup>11–17</sup> fewer studies have considered hydrophobic or uncharged polar solutes, despite their great biochemical relevance, illustrated by the large number of hydrophobic amino-acid side chains. The latter studies have essentially been devoted to determining the extent and origin of the water rotational retardation around hydrophobic groups with respect to the bulk.<sup>18,19</sup>

Here, we focus more specifically on the dynamics of the water H-bonds and investigate how the constant rearrangements of the H-bond network are affected by different amphiphilic solutes. Such molecules possess both hydrophobic and hydrophilic moieties and constitute good first models of the chemical

\* To whom correspondence should be addressed. E-mail: damien.laage@ens.fr.

<sup>†</sup> UMR ENS-CNRS-UPMC 8640.

<sup>‡</sup> University of Colorado.

heterogeneity present, for example, in an organic acid or more extensively on an exposed protein surface. Among ultrafast spectroscopy techniques, two-dimensional infrared (2D IR) vibrational echo spectroscopy has recently emerged as a very powerful tool to probe H-bond dynamics.<sup>20–22</sup> This spectroscopy measures the time dependence of the water vibrational stretch frequency, which reflects the local environment fluctuations, and has already been successfully applied to study H-bond dynamics in pure water and aqueous salt solutions.<sup>8,13,23–27</sup> As we will show within, 2D IR spectroscopy can selectively probe the water dynamics around specific solute sites through a vibrational frequency shift. This feature contrasts with most other techniques employed to study water dynamics around solutes, such as NMR,<sup>28,29</sup> quasielastic neutron scattering,<sup>30</sup> THz spectroscopy<sup>31,32</sup> or broadband ultrafast anisotropy.<sup>11–14</sup> These techniques rely on concentration-dependence studies and measure the water behavior averaged within the entire first hydration layer. 2D IR spectra yield a wealth of information, but their interpretation is often complex, especially in heterogeneous systems.<sup>20,21</sup> Molecular dynamics simulations are therefore a valuable and incisive tool to provide a molecular picture of the mechanisms reflected in the spectral dynamics. In this contribution, we report the first calculations of 2D IR spectra for aqueous solutions of amphiphiles. While the detailed dynamics of water around a solute can be readily accessed through numerical simulations, calculation of these spectra can provide a validation of these results through a direct connection to experimental data. We identify the key solute properties that modify the spectra with respect to the bulk, and evidence what these experimentally accessible spectra reveal about the molecular-scale H-bond dynamics.

The remainder of the paper is organized as follows. We first describe the simulation methodology in Section II. We then present the 2D IR spectra for a paradigm amphiphilic solute, trimethylamino-*N*-oxide in Section III before evidencing the presence of a key chemical exchange between two types of H-bond acceptors in Section IV. We then present a detailed analysis of the frequency time correlation function in Section V and discuss in Section VI the effect of exchange on the relaxation of 2D spectra for a series of amphiphilic solutes including trimethylamino-*N*-oxide, tetramethylurea, tert-butyl alcohol, and the purely hydrophobic xenon. We show in Section VII that 2D IR can distinguish between the respective influences of hydrophilic and hydrophobic groups on water dynamics, and we finish with some concluding remarks in Section VIII.

## II. Methods

**Molecular Dynamics Simulations.** We have performed classical molecular dynamics simulations of different aqueous solutions of amphiphilic solutes at different concentrations. All simulations employ the water SPC-E<sup>33</sup> model and different solute force-fields (trimethylamino-*N*-oxide (TMAO),<sup>34</sup> tetramethylurea (TMU),<sup>35</sup> tert-butyl alcohol (TBA),<sup>36</sup> and Xe<sup>37</sup>). The simulation boxes all contain a total of 500 particles at the experimental density (TMAO,<sup>38,39</sup> TMU,<sup>40</sup> TBA;<sup>41,42</sup> for Xe, no experimental density is available and the density has been estimated through NPT equilibration). The system is first equilibrated in the canonical ensemble at  $T = 298$  K for 100 ps. The trajectory is then propagated in the microcanonical ensemble for 2 ns with a 1 fs time step and periodic boundary conditions, treating the long-range electrostatic interactions through Ewald summation. The resulting average temperature is  $298 \pm 1$  K.

**Calculation of 2D IR Spectra.** Most experimental 2D IR studies of water dynamics employ an isotopic mixture of dilute HOD in either H<sub>2</sub>O or D<sub>2</sub>O to avoid certain complications due to vibrational energy transfer.<sup>20–22</sup> We chose to consider the OD stretch of dilute HOD in H<sub>2</sub>O rather than the OH stretch of HOD/D<sub>2</sub>O because of the greater relevance of H<sub>2</sub>O as a solvent, and of the longer vibrational population lifetime of the OD stretch which allows measurement of experimental spectra at longer time delays.<sup>24</sup> All the waters in our simulations are H<sub>2</sub>O molecules (and not dilute HOD in H<sub>2</sub>O) to increase the sampling. The OD stretch vibrational frequency was determined from the local electric field using the frequency map from ref 43. When the vibrational frequency is so calculated, each water stretching mode is treated as an isolated OD vibration, as would be the case in HOD. The effects of this approximation on the dynamics have been verified to be negligible.<sup>44</sup> The 2D IR vibrational echo spectra were then calculated based on the third order nonlinear response functions, including non-Condon effects, orientational and vibrational lifetime effects, and without assuming Gaussian dynamics, following the procedure detailed in refs 43 and 44.

**Calculation of Jump Times.** The jump time from one H-bond acceptor to another is defined as the average time to go from a stable H-bond with the initial acceptor to a stable H-bond with the new acceptor.<sup>19,45</sup> The jump time  $\tau$  is the inverse forward rate constant for this “reaction” process<sup>45,46</sup> and is calculated through the cross time-correlation function between the initial (I) and final (F) states as  $\langle p_I(0)p_F(t) \rangle = 1 - \exp(-t/\tau)$ , where  $p_{I,F}$  is 1 if the system is in state I (F, respectively) and 0 otherwise. States I and F are defined within the Stable States Picture<sup>47</sup> to remove the contributions from longer time barrier recrossing,<sup>19,45</sup> and absorbing boundary conditions in the product state ensure that the desired forward rate constant is calculated.

## III. 2D IR Spectra of a Paradigm Amphiphile, TMAO

The paradigm amphiphilic solute we have studied is TMAO (CH<sub>3</sub>)<sub>3</sub>N<sup>+</sup>O<sup>-</sup>, whose three methyl groups render it hydrophobic on one end, while its negatively charged oxygen makes it hydrophilic on the other end and therefore soluble in water up to high concentrations. TMAO is a protective osmolyte found, for example, in deep water fish, where it counteracts the adverse effect of high hydrostatic pressure on protein structure. Our choice was motivated by the recent experimental<sup>18,29</sup> and theoretical<sup>19</sup> work on the impact of TMAO on the reorientational dynamics of water.

We have performed classical molecular dynamics simulations of room temperature aqueous TMAO solutions of increasing concentration from 0 to 8 m and have calculated the 2D IR spectra of the OD stretch of HOD at different waiting times (see Methods). The calculated 2D IR spectra of neat HOD/H<sub>2</sub>O in the absence of TMAO (Figure 1) display the same dynamics as the experimental spectra.<sup>24</sup> At delays shorter than the frequency correlation time, which governs the time scale of the dephasing of the frequency, the frequency memory between excitation and detection is largely preserved and the 2D correlation spectrum is elongated along the diagonal. For longer delays, the positive-going band associated with the 0-1 OD vibrational transition becomes increasingly symmetrical and round due to the loss of frequency correlation.<sup>24</sup> In dilute 1 m TMAO solution (Figure 1), the spectra are very similar to neat water spectra. This evidences that very few waters are affected by the solute and thus that the solute influence on the water H-bond dynamics is short-ranged. This conclusion is in contrast

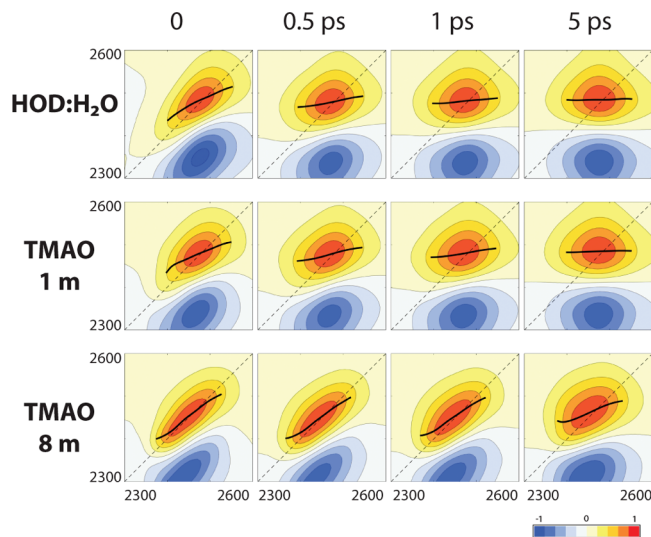


**Figure 1.** Calculated 2D IR spectra of HOD/H<sub>2</sub>O, 1 m TMAO and 8 m TMAO aqueous solutions for waiting times from 0 to 5 ps. The horizontal and vertical axes correspond respectively to the excitation and detection frequencies, both in cm<sup>-1</sup>. Each spectrum is normalized with respect to the positive peak height. The black lines show the center line slope (CLS)<sup>48</sup> on a 150 cm<sup>-1</sup> wide interval centered on the positive peak.

with those from recent THz spectroscopy experiments on other molecules<sup>31</sup> but is in agreement with pump–probe experiments.<sup>12,18</sup> The concentrated 8 m solution result is strikingly different, with the frequency correlation persisting much longer and having not fully decayed even after 5 ps (Figure 1). In the following sections, we will be concerned with the interpretation of these results. Here we describe some further general features of the spectra.

Several methods have been suggested to quantify the frequency correlation relaxation from 2D IR spectra; here we employ the CLS,<sup>48</sup> the slope of the positive peak's crest along the horizontal excitation frequency axis (see Figure 1). The CLS was shown to be equal to the normalized frequency time correlation function, which we will explicitly consider later, under certain conditions.<sup>48</sup> However, these conditions include the neglect of non-Condon effects, which have been shown to be important for water,<sup>43</sup> and the assumption that the frequency dynamics are Gaussian, which is not the case for water at short time delays.<sup>49,50</sup> Due to these restrictions, we will employ the CLS only as a convenient measure of the spectral relaxation.

The CLS time-decays exhibit a pronounced slowdown with increasing TMAO concentrations (Figure 2), especially at the 8 m highest studied concentration. Similar slowdowns of the CLS decay have been observed experimentally in concentrated NaBr aqueous solutions and interpreted as a slower spectral diffusion due to an ion-induced slowdown of the H-bond network dynamics.<sup>14</sup> While both ionic and amphiphilic solutes may slow down the water H-bond dynamics (especially in concentrated solutions), we will see that slowdown in the 2D IR spectral relaxation appears greatly enhanced with respect to the *actual* slowdown in the H-bond dynamics compared with the bulk, pure water dynamics.

#### IV. Chemical Exchange between H-Bond Acceptors

The water deuteroyl vibrational frequency that is probed by 2D IR spectra depends sensitively on the type of H-bond in which it is engaged and especially on the nature of the H-bond acceptor. When comparing the 2D IR spectra in TMAO aqueous

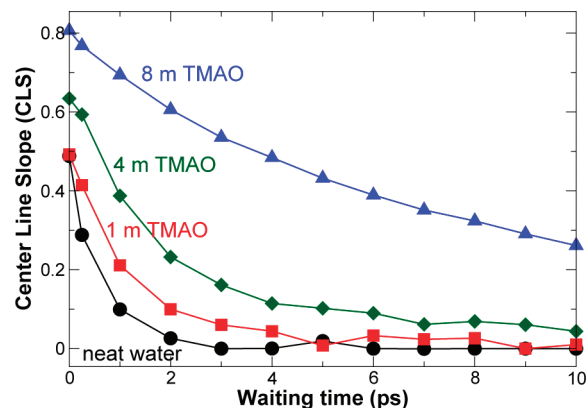


**Figure 2.** CLS<sup>48</sup> decays with the waiting time for HOD/H<sub>2</sub>O of 1, 4, and 8 m TMAO aqueous solutions. The reported CLS values are determined from a linear regression of the CLS on a 100 cm<sup>-1</sup> interval centered on the peak. Error bars are estimated to be approximately  $\pm 0.05$ . The colored lines are only guides to the eye. The initial CLS value is due to the interplay between inhomogeneous and homogeneous broadening of the 2D IR band, respectively along the spectrum diagonal and antidiagonal; for increasing TMAO concentration, the amplitude of the O<sub>TMAO</sub> peak increases, thus enhancing the inhomogeneous broadening, and leading to a larger initial CLS value.

solutions with the spectra in neat water, it is therefore critical to note the following important feature. In neat water, a single type of acceptor exists (the water oxygens O<sub>W</sub>). In contrast, in the presence of TMAO each deuteroyl can be in one of two states: it is either H-bonded to a water oxygen O<sub>W</sub> or to a hydrophilic TMAO oxygen O<sub>TMAO</sub> (transient H-bond breakings from each acceptor are included with its population). Deuteroyls vicinal to the TMAO hydrophobic groups are H-bonded to O<sub>W</sub> and thus are included within this population. Because of the strong electric field induced by the large TMAO dipole moment (5.6 D<sup>34</sup> vs 2.35 D for SPC/E H<sub>2</sub>O), O<sub>TMAO</sub> accepts strong H-bonds, which result in a 30 cm<sup>-1</sup> redshift of the OD frequency with respect to the O<sub>W</sub> acceptor case (Figure 3).<sup>51</sup> This strong H-bond formation explains the redshift of the overall IR absorption spectra for increasingly concentrated TMAO solutions, observed both experimentally<sup>52</sup> and in our simulations (Figure 3). In contrast with previous interpretation,<sup>52</sup> this redshift is thus not due to a strengthening of the water–water H-bonds in the vicinity of the TMAO hydrophobic groups but instead results from the increasing fraction of strong H-bonds with a solute hydrophilic head (see Supporting Information).

The shifted OD frequency distributions when there are H-bonds to O<sub>TMAO</sub> or O<sub>W</sub> lead to different peaks in the 2D IR spectra and imply that exchanges between the two types of H-bond acceptors should be visible in the frequency dynamics and thus in the 2D IR spectra, as now discussed.

In 2D IR spectra, chemical exchange between two states usually manifests itself through the presence of two distinct diagonal peaks and the growth of off-diagonal peaks.<sup>13,20,21,53,54</sup> But here, these characteristic signatures are not discernible for two reasons. First, it is because the two frequency distributions are too close to be distinguished in the spectra, leading to one broad peak, and second, because the exchange time scale, calculated to be >10 ps from our simulations (Figure 4), is too slow to be observed during the limited time window imposed by the 1.5 ps OD vibrational lifetime.<sup>24</sup> Nonetheless, as we will see, exchange is essential to correctly interpret these 2D IR spectra and the origin of the relaxation slower than in neat water.



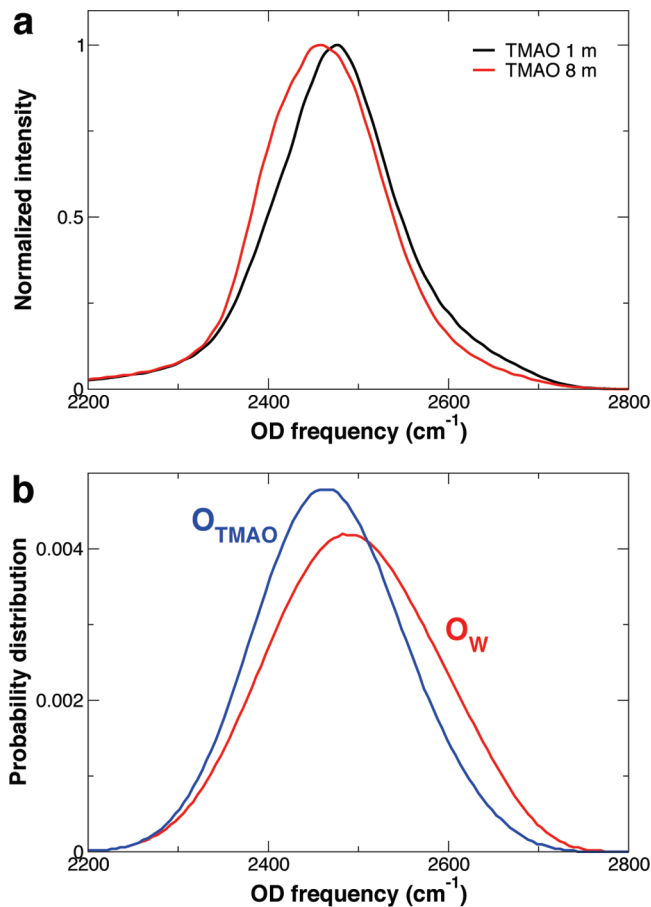


**Figure 3.** (a) Linear infrared spectrum of 1 and 8 m TMAO aqueous solutions; (b) frequency distribution for  $O_W$  and  $O_{TMAO}$  acceptors in the 8 m TMAO aqueous solution.

## V. Frequency Time Correlation Function (ftcf)

Further insight into the mechanisms underlying the 2D IR spectral decay and the actual effect of the solute on the water frequency dynamics is brought by the direct computation of the ftcf

$$C(t) = \langle \delta\omega(0)\delta\omega(t) \rangle \quad (1)$$

where  $\delta\omega(t)$  is the difference between the instantaneous<sup>47</sup> OD frequency at time  $t$  and the time-averaged frequency. As noted in Section III,  $C(t)$  is a measure of the dephasing time for the OD frequency, and when normalized by its initial time value, is approximately related to the CLS in the 2D IR spectrum.<sup>48</sup> We calculate the ftcf, distinguishing whether OD is initially H-bonded to  $O_W$  or  $O_{TMAO}$  (Figure 4a). In both cases, the frequency first relaxes very rapidly through an  $\sim 100$  fs librational contribution, followed by an approximate  $\sim 1$  ps intermediate decay, which has been shown in bulk water<sup>49,50,55</sup> and for anions in water<sup>13</sup> to result from transient H-bond breaking and making.<sup>49,50,55</sup> Since this dephasing is faster than exchange (Figure 4b), it occurs with OD next to its initial acceptor. We pause to discuss this intermediate decay.

**ftcf Intermediate Time Decay.** We compare the intermediate decay times for the following three situations: ODs H-bonded to the TMAO hydrophilic site, ODs H-bonded to water lying around the TMAO hydrophobic groups, or ODs in the bulk (data not shown). The intermediate decay time is found to depend on the nature of the H-bond acceptor; it is slightly longer for

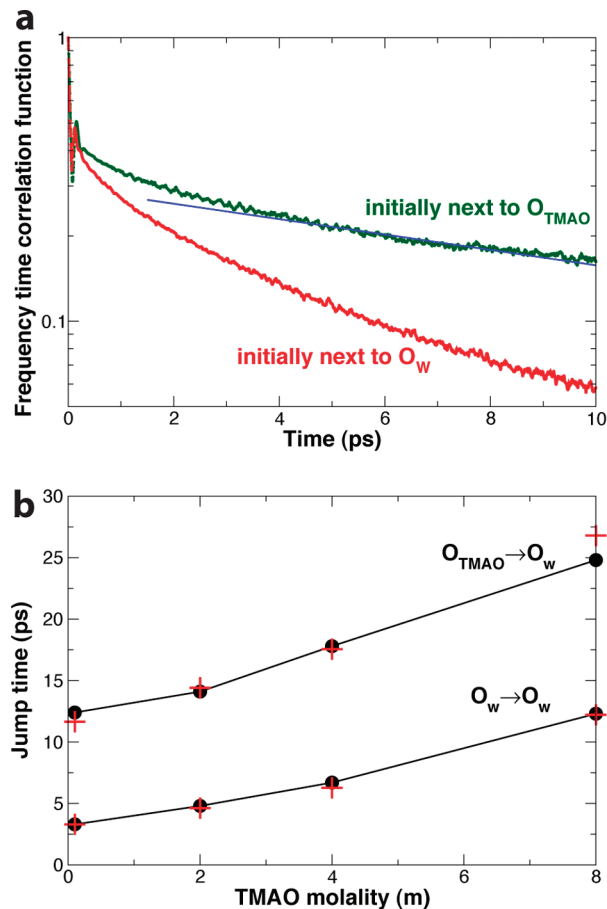


**Figure 4.** (a) Frequency time correlation function decay in 8 m TMAO aqueous solution for a deuteroyl initially hydrogen-bonded either to a water oxygen  $O_W$  or a TMAO oxygen  $O_{TMAO}$ . The blue line shows the exchange contribution (see Supporting Information) with the exchange time calculated from the jump times below. (b) Calculated jump times between H-bond acceptors as a function of TMAO molality, determined from the simulations (black dots) and from our model (red crosses). Within our model, the  $O_W \rightarrow O_W$  jump time retardation factor is entirely described by the transition state excluded volume factor<sup>19</sup>  $\rho_V$  (eq 4), while the  $O_{TMAO} \rightarrow O_W$  retardation factor is assumed to be the product (eq 5) of a transition state excluded volume factor  $\rho_V$  (distinct from the  $O_W \rightarrow O_W$  one) with a concentration-independent H-bond strength factor<sup>57</sup>  $\rho_{HB}$  (eq 3), taken here to be 2.8.

H-bond donors to  $O_{TMAO}$  than for donors to  $O_W$  (1.25 ps for  $O_{TMAO}$  vs 0.9 ps for  $O_W$  in dilute 0.1 m TMAO), because the first H-bond is stronger and transient breakings occur less frequently.<sup>56</sup> In contrast, the hydrophobic TMAO methyl groups are not observed to affect the surrounding water frequency dynamics; in dilute solutions, the intermediate decay time for these ODs is similar to that in the bulk. This analysis shows that the slowdown induced by dilute TMAO on the vibrational dephasing time of the surrounding waters, and thus in their transient H-bond breaking kinetics, is limited to the waters H-bonded to the hydrophilic head, and that this retardation factor is moderate (approximately 1.25 ps/0.9 ps  $\sim 1.4$ ). The consequence for the 2D IR spectra is that each diagonal peak decays on an approximate picosecond time scale to a round shape, in a fashion similar to bulk water; however, this is not reflected in the CLS, because the sum of these two close diagonal peaks leads to a persistent elliptic band, elongated along the diagonal.<sup>20</sup>

**ftcf Longer Time Decay and Exchange.** We now turn to a discussion of the longer time behavior. In contrast with neat water, in TMAO solutions both the  $O_W$  and  $O_{TMAO}$  ftcfs (and the CLS) exhibit an additional, long-time decay past  $\sim 1$  ps

(Figure 4a). This slow component is due to chemical exchange between the two populations, which is necessary for the OD to sample all environments (especially both types of H-bond acceptors), and for its frequency to reach a full decorrelation, as shown quantitatively in Supporting Information. This is analogous to the case of water in ionic solutions, where the ftcf and 2D IR spectra slow component has been assigned to an exchange between the anion hydration shell and the bulk.<sup>13,15</sup> This component is absent in pure water, where only a single H-bond acceptor type exists. The slow decay time  $\tau_{ex}$  due to exchange results from the forward and backward exchange times between the  $O_W$  and  $O_{TMAO}$  states, (see Supporting Information)

$$\tau_{ex} = 1/(1/\tau_{TMAO \rightarrow W} + 1/\tau_{W \rightarrow TMAO}) \quad (2)$$

and we now detail how these times can be determined.

Our simulations indicate that acceptor exchanges from one  $O_{TMAO}$  to another  $O_{TMAO}$  are negligible, even at high TMAO concentration, and the  $\tau_{TMAO \rightarrow W}$  chemical exchange time from the  $O_{TMAO}$  to the  $O_W$  population is therefore equal to the H-bond jump time between these two acceptors. The jump time is defined as the time to replace a stable H-bond with an initial acceptor by a stable H-bond with a new acceptor.<sup>16,19,45,46</sup> The backward exchange time then follows from the equilibrium constant  $K = \tau_{TMAO \rightarrow W}/\tau_{W \rightarrow TMAO}$  between the two populations.

The  $\tau_{TMAO \rightarrow W}$  jump time can be calculated from our simulations using the procedure detailed in ref 45 (see also Methods) and is found to be slower than the jump time between two  $O_W$  acceptors by a factor of approximately 4 in dilute solutions (Figure 4b). We recently showed that this retardation originates from a combination of two effects.<sup>57</sup> The first is an H-bond strength effect, which is approximately concentration-independent. The initial  $OD \cdots O_{TMAO}$  H-bond is stronger than the  $OD \cdots O_W$  H-bond ( $O_{TMAO}$  is more hydrophilic than  $O_W$  due to the TMAO large dipole moment); since its elongation is part of the rate-limiting step to reach the transition state in the acceptor exchange mechanism,<sup>45</sup> this process is more energetically expensive and therefore more unfavorable. The slowdown with respect to the bulk is<sup>57</sup>

$$\rho_{HB} = \exp[(\Delta G_{TMAO}^\ddagger - \Delta G_W^\ddagger)/RT] \quad (3)$$

where  $\Delta G_{TMAO,W}^\ddagger$  are the free energy costs to stretch the initial H-bond with  $O_{TMAO}$  ( $O_W$  respectively) to its transition state length.

The second effect stems from the solute-induced transition state excluded volume fraction, which increases markedly with the solute concentration. As we previously showed, the presence of a hydrophobic group blocks the approach of some new  $O_W$  H-bond acceptors, thus retarding the jump rate between H-bond acceptors for waters around hydrophobic groups.<sup>19</sup> The jump time increase with increasing solute concentration is quantitatively described (Figure 4b) by the transition state excluded volume model we have previously developed.<sup>19</sup> The slowdown factor with respect to the bulk is<sup>19</sup>

$$\rho_v = 1/(1 - f) \quad (4)$$

where  $f$  is the fraction of transition state locations for the new acceptor which are forbidden by the solute's presence. The resulting jump time is then

$$\tau = \rho_{HB} \rho_v \tau_{W \rightarrow W}^{bulk} \quad (5)$$

where  $\tau_{W \rightarrow W}^{bulk}$  is the jump time in the bulk between two water oxygen acceptors.

With the inclusion of the above two effects, the resulting exchange time  $\tau_{ex}$  determined from this  $\tau_{TMAO \rightarrow W}$  jump time in the 8 m TMAO solution (and from the  $\tau_{W \rightarrow TMAO}$  time inferred from the 8 m equilibrium constant  $K = \tau_{TMAO \rightarrow W}/\tau_{W \rightarrow TMAO} \approx 3.1$ ) is shown to describe very well the long-time decay of the ftcf in Figure 4a (see also Methods).<sup>58</sup>

The amplitude of the exchange-governed slow ftcf decay is seen in Figure 4a to be much greater for waters initially bonded to  $O_{TMAO}$  than for those bonded to  $O_W$ . This is because the initial frequency of the former waters differs more from the average frequency, which is dominated by the more abundant  $O_W$  acceptors (76% at 8 m) (a quantitative derivation is provided in Supporting Information).

## VI. Effect of Exchange on 2D Spectral Relaxation

Provided with the preceding section's results on the water frequency dynamics, we now return to the interpretation of the 2D IR spectra. While the slowly decaying elliptic band in the 2D IR spectra of amphiphilic solutions strongly resembles the neat water spectra at early delays before dephasing has occurred (Figure 1), the decay mechanisms of these bands are totally different, and their relaxation times cannot be legitimately compared, as now discussed.

**TMAO and Neat Water Spectra.** The decay of the neat water spectra in Figure 1 is due to transient H-bond-breaking and -making events<sup>24,25,49,50,55</sup> as shown by our ftcf analysis in Section V, this contribution is also present in solutions of amphiphiles, as seen through the increase in the antidiagonal line width. However, in concentrated solutions of amphiphiles, the long-lived elliptic band results, as discussed in Section V, from the sum of two close peaks along the diagonal and its decay is governed by exchanges between these two peaks (see Supporting Information), corresponding to the two types of H-bond acceptors (water and the solute hydrophilic group). The very pronounced slowdown of the spectral dynamics with increasing solute concentration seen in the CLS decay (Figure 2) and in the 2D IR spectra (Figure 1) originates from the increasing fraction of the  $O_{TMAO}$  waters, together with the jump time lengthening with the hydrophilic  $O_{TMAO}$  concentration due to the increased difficulty to find a water acceptor, as discussed in detail in Section V (Figure 4b).

We pause to note that the slow exchange between the  $O_{TMAO}$  and  $O_W$  populations implies that even at long delays, the frequency dynamics in these heterogeneous solutions is non-Gaussian, and the CLS is therefore not strictly equal to the ftcf (see the comparison at different concentrations in Supporting Information). However, the CLS still provides a useful measure of the slow relaxation of the 2D IR spectra, since its long-time decay yields the exchange time scale  $\tau_{ex}$ , as shown in Supporting Information.

The question arises as to the proper comparison to provide a perspective for the slow decay time of the 2D IR spectra. In view of our identification above of this decay with exchange, the comparison should not be made with the bulk water ftcf dephasing time (1.5 ps for HOD/H<sub>2</sub>O<sup>24</sup>), which does not reflect H-bond exchange since the exchanging states have the same frequency. Instead the proper comparison is with the bulk H-bond acceptor exchange time. This latter exchange between two water oxygens cannot be observed in 2D IR, just as in the

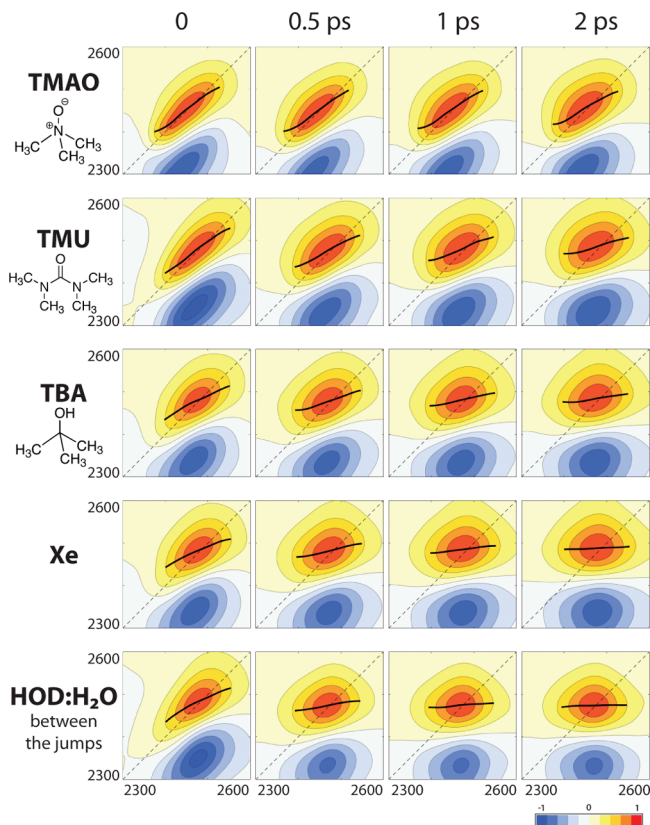


**Figure 5.** Calculated 2D IR spectra of concentrated 8 m solutions of TMAO, TBA,<sup>59</sup> TMU, and Xe aqueous solutions. The bottom row shows the spectra for HOD/H<sub>2</sub>O calculated between hydrogen-bond acceptor jumps. The horizontal and vertical axes correspond respectively to the excitation and detection frequencies, both in cm<sup>-1</sup>. These spectra are normalized as in Figure 1 and the black lines show the center line slope<sup>48</sup> in the center of the positive band. Several of these solutes (TBA, TMU, Xe) aggregate in aqueous solution,<sup>36,67</sup> and the fraction of water next to a solute is not proportional to the concentration, but this does not affect our conclusions.

ftcf, for the same reason. However, it has been calculated to be 3.3 ps at 300 K.<sup>45</sup> As detailed in Section V, comparison of the slow spectral decay time with this bulk exchange time yields a measure of the hydrophilic site's influence on the water H-bond dynamics.

The solute concentration dependence of the exchange contribution to the 2D IR spectra decay (both its amplitude and time scale, see Supporting Information and ref 19) is pronounced and cannot be ignored. As shown in Figure 4b, the exchange time depends sensitively on the solute concentration, and the influence of an isolated solute on water dynamics cannot be straightforwardly inferred from the experimental results on concentrated solutions.

**2D IR Spectra of Other Solutes.** The critical role of the hydrophilic group in determining the 2D IR spectral relaxation is further substantiated by examining the spectra for a series of concentrated amphiphilic solutes, shown in Figure 5. For TMU, whose hydrophobic moiety comprises two methyl group pairs, the hydrophilic head is a carbonyl function, which is a weaker H-bond acceptor than water, and thus shifts the deuteroyl frequency to the blue (see Supporting Information). The 2D spectra therefore shift to the blue for increasing TMU concentration, but this does not alter the basic effect of chemical exchange, which is analogous to the TMAO case, also shown in Figure 5, leading to a long-lived elliptical shape. For TBA, the hydrophilic head is a hydroxyl group, which induces a very

limited frequency-shift with respect to the bulk; the frequency distributions in the two populations, H-bonded to a water and H-bonded to the solute, are similar (see Supporting Information), and the two diagonal peaks are superimposed. The resulting spectral relaxation (Figure 5)<sup>59</sup> is dramatically faster than for TMAO (where the frequency shift is larger); this evidences that frequency dephasing is not significantly retarded within each population. Since the hydrophobic side of TBA is identical to that of TMAO, that is, three methyl groups, this clearly shows that the slow dynamics in TMAO solutions is not due to the hydrophobic groups but instead arises from exchange involving the hydrophilic head. This general feature is definitively confirmed by the spectra of Xe aqueous solutions (Figure 5). In the absence of any hydrophilic group, no frequency shift with respect to the bulk is observed. This indicates that hydrophobic groups' effect on the water vibrational frequency is negligible, and the 2D IR spectra relax nearly as fast as in the bulk, thereby also showing that the hydrophobic solute has a very limited influence on the surrounding water H-bond dynamics.

Very recently, after this work was completed, experimental 2D IR spectra for TMAO<sup>60</sup> and TMU<sup>61</sup> in water have been presented. The concentrated solutions exhibit the same retarded spectral relaxation with respect to bulk water as our calculated spectra (Figure 5). This shows that while the details of the spectra discussed are obviously sensitive to some degree to the specific force field employed, the calculated spectra reproduce the behavior observed in the experimental spectra; in addition, the comparison between solutes described with very different force fields shows that the overall effect is force-field independent.

The retarded spectral relaxation observed in the experimental spectra was interpreted as revealing the dramatic slowdown in the water dynamics induced by the hydrophobic groups, due to the suppression of water jumps between H-bond acceptors.<sup>60,61</sup> As we just showed, this interpretation is not at all appropriate; the critical role of the solute hydrophilic group and the resulting chemical exchange cannot be ignored as in refs 60 and 61 and the slower spectral relaxation is not due to the hydrophobic groups but instead is due to the hydrophilic one. We will also show below that this slowdown is not due to a suppression of jumps and that 2D IR spectra do not support a picture of immobilized waters around hydrophobic groups.

## VII. 2D IR Separates the Hydrophilic and Hydrophobic Influences on Water Dynamics

Prior NMR<sup>29</sup> and time-resolved anisotropy<sup>18</sup> experiments on water dynamics around amphiphilic solutes could not directly discriminate the respective roles of hydrophobic and hydrophilic moieties. In contrast, the present work shows that 2D IR spectroscopy can specifically probe water dynamics around hydrophilic groups when their deuteroyl frequency distribution differs from the bulk, while waters around hydrophobic groups appear together with the bulk because their vibrational frequency is similar.

Furthermore, 2D IR spectroscopy can provide an experimental estimate for the exchange time scale between the hydrophilic site and the bulk. Our simulations show that for dilute TMAO, the acceptor exchange time is slowed down by a factor of approximately 4 by the hydrophilic group (Figure 4b). The exchange time between the vicinity of a hydrophobic group and the bulk cannot be determined from the 2D IR spectra. However, through simulations, we previously determined this exchange time to be moderately slowed down at low concentration by a factor  $\sim 1.5$ <sup>19</sup> with respect to the bulk, a result supported by



NMR experiments<sup>29</sup> and recent first principles simulations.<sup>62</sup> This again underscores the importance of the hydrophilic group, not only in the interpretation of 2D IR spectra as detailed above, but also at a molecular scale for the impact of an amphiphilic solute on the surrounding water dynamics.

A further implication of the present results is that, since H-bond acceptor exchange has been shown elsewhere to be the main water reorientation pathway,<sup>16,19,45,46,57</sup> water reorientation is most retarded around the hydrophilic groups. Accordingly, the assumption used in the interpretation of time-resolved anisotropy experiments<sup>18</sup> that hydrophilic groups do not perturb the water dynamics and can be ignored is not at all appropriate, especially at the high 8 m concentration employed experimentally.<sup>18</sup>

The anisotropy experiments just referred to were interpreted as indicating that hydrophobic groups strongly suppress the jumps between acceptors for waters in their vicinity (indeed, such water molecules were described as “immobilized”)<sup>18</sup> while simulations showed that no immobilization occurs and that these jumps are only moderately retarded.<sup>19</sup> We now investigate what contribution 2D IR can bring to this specific issue of hydrophobic hydration dynamics.

Around hydrophobic groups, waters jump between similar  $O_W$  acceptors,<sup>19</sup> leading to similar vibrational frequencies, and accordingly this particular exchange process cannot be directly observed through 2D IR. The suppression of water jumps by hydrophobic groups suggested in ref 18 was claimed to be the cause of the retarded 2D IR spectral relaxation in the presence of hydrophobic groups.<sup>61</sup> If this were the case, the water 2D IR spectra in the presence of a hydrophobic solute should be similar to the pure water spectra in the absence of jumps. To examine this issue, we have calculated such spectra for HOD/H<sub>2</sub>O, by focusing on the simulation time intervals between the jumps, without modifying the simulation. The resulting spectra (Figure 5) are extremely similar to the regular 2D IR water spectra (Figure 1) and do not exhibit any retarded relaxation. This shows that 2D IR spectra do not support the hydrophobic immobilization picture. This conclusion also follows from our calculated spectra for the purely hydrophobic solute Xe (Figure 5), which showed that water frequency dynamics is not noticeably affected by such solutes.

Beyond the specific issue of hydrophobic hydration, the neat water spectra in the absence of jumps more generally evidence that water 2D IR spectral dynamics is mostly determined by transient H-bond breakings, corresponding to unsuccessful jumps, in agreement with previous work.<sup>49,50,55</sup> In contrast with anisotropy measurements which are selectively sensitive to the successful jumps because only they result in a stable reorientation, 2D IR follows the frequency dynamics, which cannot discriminate whether a transiently broken H-bond deuteroyl returns to its initial acceptor or forms an H-bond with a new acceptor, except when these two acceptors induce different OD vibrational frequency shifts.

### VIII. Concluding Remarks

Through the study of a series of amphiphilic solutes in aqueous solutions, we have evidenced that the effect of these solutes on the surrounding water dynamics mostly originates from the hydrophilic groups. Through the formation of strong hydrogen-bonds with water, these groups can retard the water dynamics much more significantly than hydrophobic sites that only moderately slow down the water dynamics via an excluded volume effect.

These conclusions, based on molecular dynamics simulations and analytic modeling, have been connected to experimentally

accessible two-dimensional infrared photon echo data through the calculation of the two-dimensional spectra. We have evidenced that while this technique is very powerful to probe the hydrogen-bond network fluctuations, numerical simulations are extremely valuable to correctly interpret these spectra and lift ambiguities, especially in heterogeneous solutions. We have shown that two-dimensional infrared spectroscopy can provide unprecedented information on the hydration layer dynamics through the measurement of the water exchange time between hydrophilic sites and the rest of the solution. When an H-bond acceptor hydrophilic site shifts the water vibrational frequency, this results in two populations with H-bond donation either to the hydrophilic group or to another water. The exchange kinetics of these populations determines the spectral relaxation time, even when the usual features of chemical exchange are not discernible in the 2D IR spectra. Finally, our calculated 2D IR spectra on a series of solutes evidence that hydrophobic groups induce a very modest slowdown of the water vibrational frequency dynamics, in accord with previous results on the orientational relaxation and stable H-bond exchanges.<sup>19</sup>

The present results indicate that around chemically heterogeneous solutes such as proteins, whose solvent-exposed surfaces alternate between hydrophilic and hydrophobic sites, hydrophilic H-bond acceptor sites (such as carboxylate end groups<sup>57</sup>) are likely to have the greatest influence on the water dynamics. A study of hydration dynamics around a protein is currently underway in our group to examine this issue. Our present work also provides guidelines for the difficult interpretation of 2D IR spectra in aqueous solutions, which should prove valuable for the challenging study of water next to assorted biomolecules. Around hydrophilic H-bond acceptor sites inducing a frequency shift in the water vibration with respect to the bulk (such as the DNA phosphate groups<sup>63</sup>), 2D IR spectroscopy can be expected to provide an unprecedented detailed observation of the water dynamics, and especially of the exchange time scale between the hydration layer and the bulk.<sup>64–66</sup>

**Acknowledgment.** Fabio Sterpone is gratefully acknowledged for his help with the retardation factor calculations. We thank Jim Skinner (University of Wisconsin, Madison) for enlightening discussions on the calculation of 2D IR spectra and Maxim Pshenichnikov (Gröningen) for showing us the TMAO 2D IR spectra before publication. This work was supported in part by NSF Grant CHE-0750477 (J.T.H.).

**Supporting Information Available:** Supporting Information includes (1) the calculated infrared spectra for TMAO solutions of increasing concentration, (2) the frequency distribution for  $O_W$  and  $O_{\text{solute}}$  acceptors in 8 m TMAO, TMU, and TBA solutions, (3) the comparison between Center Line Slope and frequency time correlation function for different TMAO concentrations, (4) the analytic expression for the ftcf decay in the presence of chemical exchange, and (5) the analytic expression for the CLS decay in the presence of chemical exchange. This material is available free of charge via the Internet at <http://pubs.acs.org>.

### References and Notes

- (1) Gertner, B. J.; Whitnell, R. M.; Wilson, K. R.; Hynes, J. T. *J. Am. Chem. Soc.* **1991**, *113*, 74.
- (2) Ando, K.; Hynes, J. T. *J. Mol. Liq.* **1995**, *64*, 25.
- (3) Ando, K.; Hynes, J. T. *J. Phys. Chem. B* **1997**, *101*, 10464.
- (4) Agmon, N. *Chem. Phys. Lett.* **1995**, *244*, 456.
- (5) Marx, D.; Tuckerman, M. E.; Hutter, J.; Parrinello, M. *Nature* **1999**, *397*, 601.
- (6) Ball, P. *Chem. Rev.* **2008**, *108*, 74.

- (7) Garczarek, F.; Gerwert, K. *Nature* **2006**, *439*, 109.
- (8) Elsaesser, T. *Acc. Chem. Res.* **2009**, *42*, 1220.
- (9) Levy, Y.; Onuchic, J. N. *Annu. Rev. Biophys. Biomol. Struct.* **2006**, *35*, 389.
- (10) Kimura, T.; Maeda, A.; Nishiguchi, S.; Ishimori, K.; Morishima, I.; Konno, T.; Goto, Y.; Takahashi, S. *Proc. Natl. Acad. Sci. U.S.A.* **2008**, *105*, 13391.
- (11) Kropman, M. F.; Bakker, H. J. *Science* **2001**, *291*, 2118.
- (12) Omta, A. W.; Kropman, M. F.; Woutersen, S.; Bakker, H. J. *Science* **2003**, *301*, 347.
- (13) Moilanen, D. E.; Wong, D.; Rosenfeld, D. E.; Fenn, E. E.; Fayer, M. D. *Proc. Natl. Acad. Sci. U.S.A.* **2009**, *106*, 375.
- (14) Park, S.; Fayer, M. D. *Proc. Natl. Acad. Sci. U.S.A.* **2007**, *104*, 16731.
- (15) Nigro, B.; Re, S.; Laage, D.; Rey, R.; Hynes, J. T. *J. Phys. Chem. A* **2006**, *110*, 11237.
- (16) Laage, D.; Hynes, J. T. *Proc. Natl. Acad. Sci. U.S.A.* **2007**, *104*, 11167.
- (17) Lin, Y. S.; Auer, B. M.; Skinner, J. L. *J. Chem. Phys.* **2009**, *131*, 144511.
- (18) Rezus, Y. L. A.; Bakker, H. J. *Phys. Rev. Lett.* **2007**, *99*, 148301.
- (19) Laage, D.; Stirnemann, G.; Hynes, J. T. *J. Phys. Chem. B* **2009**, *113*, 2428.
- (20) Kim, Y. S.; Hochstrasser, R. *J. Phys. Chem. B* **2009**, *113*, 8231.
- (21) Zheng, J.; Kwak, K.; Fayer, M. D. *Acc. Chem. Res.* **2007**, *40*, 75.
- (22) Mukamel, S. *Principles of Nonlinear Optical Spectroscopy*; Oxford University Press: New York, 1995.
- (23) Cowan, M. L.; Bruner, B. D.; Huse, N.; Dwyer, J. R.; Chugh, B.; Nibbering, E. T. J.; Elsaesser, T.; Miller, R. J. D. *Nature* **2005**, *434*, 199.
- (24) Asbury, J. B.; Steinel, T.; Stromberg, C.; Corcelli, S. A.; Lawrence, C. P.; Skinner, J. L.; Fayer, M. D. *J. Phys. Chem. A* **2004**, *108*, 1107.
- (25) Eaves, J. D.; Loparo, J. J.; Fecko, C. J.; Roberts, S. T.; Tokmakoff, A.; Geissler, P. L. *Proc. Natl. Acad. Sci. U.S.A.* **2005**, *102*, 13019.
- (26) Loparo, J. J.; Roberts, S. T.; Tokmakoff, A. *J. Chem. Phys.* **2006**, *125*, 194522.
- (27) Park, S.; Moilanen, D. E.; Fayer, M. D. *J. Phys. Chem. B* **2008**, *112*, 5279.
- (28) Hertz, H. G.; Zeidler, M. D. *Ber. Bunsen-Ges.* **1964**, *68*, 821.
- (29) Qvist, J.; Halle, B. *J. Am. Chem. Soc.* **2008**, *130*, 10345.
- (30) Russo, D.; Hura, G.; Head-Gordon, T. *Biophys. J.* **2004**, *86*, 1852.
- (31) Heugen, U.; Schwaab, G.; Brundermann, E.; Heyden, M.; Yu, X.; Leitner, D. M.; Havenith, M. *Proc. Natl. Acad. Sci. U.S.A.* **2006**, *103*, 12301.
- (32) Kim, S. J.; Born, B.; Havenith, M.; Gruebele, M. *Angew. Chem.* **2008**, *47*, 6486.
- (33) Berendsen, H. J. C.; Grigera, J. R.; Straatsma, T. P. *J. Phys. Chem.* **1987**, *91*, 6269.
- (34) Paul, S.; Patey, G. N. *J. Phys. Chem. B* **2006**, *110*, 10514.
- (35) Belletato, P.; Freitas, L. C. G.; Areas, E. P. G.; Santos, P. S. *Phys. Chem. Chem. Phys.* **1999**, *1*, 4769.
- (36) Lee, M. E.; van der Vegt, N. F. A. *J. Chem. Phys.* **2005**, *122*, 114509.
- (37) Straatsma, T. P.; Berendsen, H. J. C.; Postma, J. P. M. *J. Chem. Phys.* **1986**, *85*, 6720.
- (38) Zou, Q.; Bennion, B. J.; Daggett, V.; Murphy, K. P. *J. Am. Chem. Soc.* **2002**, *124*, 1192.
- (39) Kast, K. M.; Brickmann, J.; Kast, S. M.; Berry, R. S. *J. Phys. Chem. A* **2003**, *107*, 5342.
- (40) Patil, K. J.; Sargar, A. M.; Dagade, D. H. *Indian J. Chem. A* **2002**, *41*, 1804.
- (41) Broadwater, T. L.; Kay, R. L. *J. Phys. Chem.* **1970**, *74*, 3802.
- (42) Nakanishi, K.; Kato, N.; Maruyama, M. *J. Phys. Chem.* **1967**, *71*, 814.
- (43) Schmidt, J. R.; Corcelli, S. A.; Skinner, J. L. *J. Chem. Phys.* **2005**, *123*, 044513.
- (44) Schmidt, J. R.; Roberts, S. T.; Loparo, J. J.; Tokmakoff, A.; Fayer, M. D.; Skinner, J. L. *J. Chem. Phys.* **2007**, *341*, 143.
- (45) Laage, D.; Hynes, J. T. *J. Phys. Chem. B* **2008**, *112*, 14230.
- (46) Laage, D.; Hynes, J. T. *Science* **2006**, *311*, 832.
- (47) Northrup, S. H.; Hynes, J. T. *J. Chem. Phys.* **1980**, *73*, 2700.
- (48) Kwak, K.; Rosenfeld, D. E.; Fayer, M. D. *J. Chem. Phys.* **2008**, *128*, 204505.
- (49) Rey, R.; Moller, K. B.; Hynes, J. T. *J. Phys. Chem. A* **2002**, *106*, 11993.
- (50) Moller, K. B.; Rey, R.; Hynes, J. T. *J. Phys. Chem. A* **2004**, *108*, 1275.
- (51) The greater strength of water–TMAO H-bonds compared to that of water–water bonds leads to a reduced structural variety, for example, smaller amplitude bond length fluctuations. The width of the water–TMAO frequency distribution would then be expected to be more narrow than that of water–water bonds. However, as shown in Figure 3b both distributions display comparable widths, because the water–TMAO structural fluctuations occur in the much stronger electric field induced by the large TMAO dipole moment associated with the  $N^+-O^-$  partial charges. While the water–TMAO structural fluctuations are reduced compared to those in bulk water, the electric field fluctuations are thus comparable, leading to similar frequency distribution widths.
- (52) Sharp, K. A.; Madan, B.; Manas, E.; Vanderkooi, J. M. *J. Chem. Phys.* **2001**, *114*, 1791.
- (53) Dlott, D. D. *Science* **2005**, *309*, 1333.
- (54) Park, S.; Odellius, M.; Gaffney, K. J. *J. Phys. Chem. B* **2009**, *113*, 7825.
- (55) Lawrence, C. P.; Skinner, J. L. *J. Chem. Phys.* **2003**, *118*, 264.
- (56) This decay time also lengthens with increasing TMAO concentration due to the same excluded volume effect as the long exchange timescale.
- (57) Sterpone, F.; Stirnemann, G.; Hynes, J. T.; Laage, D. *J. Phys. Chem. B* **2010**, *114*, 2083.
- (58) Because the equilibrium constant  $K$  is always larger than one, even in the very concentrated 8 m solution, the exchange time is dominated by the shorter  $\tau_{TMAO-W}$  jump time.
- (59) For TBA, the experimental spectra include a contribution from the solute hydroxyl. However, we have only considered the water contributions in the presented spectra to allow a meaningful comparison of the water dynamics with the other solutes.
- (60) Pschenichnikov, M. private communication.
- (61) Bakulin, A. A.; Liang, C.; Jansen, T. I. C.; Wiersma, D. A.; Bakker, H. J.; Pschenichnikov, M. S. *Acc. Chem. Res.* **2009**, *42*, 1229.
- (62) Silvestrelli, P. L. *J. Phys. Chem. B* **2009**, *113*, 10728.
- (63) Szyz, L.; Dwyer, J. R.; Nibbering, E. T. J.; Elsaesser, T. *Chem. Phys.* **2009**, *357*, 36.
- (64) Halle, B. *Philos. Trans. R. Soc. London, Ser. B* **2004**, *359*, 1207.
- (65) Pal, S. K.; Zewail, A. H. *Chem. Rev.* **2004**, *104*, 2099.
- (66) Bagchi, B. *Chem. Rev.* **2005**, *105*, 3197.
- (67) Almasy, L.; Len, A.; Szekeley, N. K.; Plestil, J. *Fluid Phase Equilib.* **2007**, *257*, 114.